

The density profiles of hot galactic halo gas

Steen H. Hansen¹ & Jesper Sommer-Larsen²

¹ *University of Zurich, Winterthurerstrasse 190, 8057 Zurich, Switzerland*

² *Dark Cosmology Centre, Niels Bohr Institute, University of Copenhagen, Juliane Maries Vej 30, DK-2100 Copenhagen, Denmark*

ABSTRACT

Extended gas haloes around galaxies are a ubiquitous prediction of galaxy formation scenarios. However, the density profiles of this hot halo gas is virtually unknown, although various profiles have been suggested on theoretical grounds. In order to quantitatively address the gas profile, we compare galaxies from direct cosmological simulations with analytical solutions of the underlying gas equations. We find remarkable agreement between simulations and theoretical predictions. We present an expression for this gas profile with a non-trivial dependence on the total mass profile. This expression is useful when setting up equilibrium galaxy models for numerical experiments.

1. INTRODUCTION

Standard galaxy formation scenarios predict that the galaxies have an extended halo of hot gas. This hot gas is gravitationally trapped by the dark matter potential and cools slowly due to thermal emission (White & Frenk 1991).

These haloes of hot gas have been observed around massive elliptical galaxies through their X-ray emission (e.g. Matsushita 2001), and recently around normal quiescent spiral galaxies (Pedersen et al. 2006). These observations provide strong support for the standard galaxy formation scenario.

One missing aspect is the qualitative understanding of the density profile of these hot haloes. We therefore investigate the density profiles extracted from virialized galaxies in cosmological simulations, as well as theoretical predictions based on the fundamental gas equations. We find remarkable agreement between simulations and theory. We present an analytical expression for the gas-profile, which depends non-trivially on the total mass distribution of both baryons and dark matter.

2. Theoretical predictions

Galaxies are dynamically old and should therefore have reached a quasi-static equilibrium state. In this state there is very little radial bulk-motion of the hot halo gas, possibly except for the very central region where cooling is important.

Since the gas has frequent collisions, then we must treat it through the Navier-Stokes equation (N-S). The N-S equations apply to any collisional gas or fluid, and are 3 hydrodynamical equations for the velocity vector. The galaxies have reached a quasi-static equilibrium state, and then the N-S equations simplify considerably since all the time-dependent terms disappear.

One of the N-S equations is the one related to the radial velocity component, and if the rotation of the gas is negligible then it reduces to the normal equation for hydrostatic equilibrium. From this equation it is straight forward to show that when the mass is dominated by a spherical distribution of matter, then the spherical gas density profile is given as a function of the underlying total matter distribution¹. One finds that everywhere throughout the galaxy the logarithmic derivative

¹One can show that there are only two asymptotic solutions to the N-S equations for the gas, one being a spherical distribution, and one being a disks (Hansen & Stadel 2003).

of the gas density

$$\beta_{gas} \equiv \frac{\partial \log \rho_{gas}}{\partial \log r}, \quad (1)$$

is given as a function of the logarithmic derivative of the total density, β_{tot} and the polytropic index, γ , which is related to the derivative of the temperature through

$$\gamma = 1 + \frac{\partial \log T}{\partial \log \rho}. \quad (2)$$

One finds the connection

$$\beta_{gas} = \kappa (\beta_{tot} + 2), \quad (3)$$

where the pre-factor is defined as $\kappa = 1/(\gamma - 1)$. In general γ can be in the range, $1 \leq \gamma \leq 5/3$, and when $\gamma = 1.5$ we have the connection, $\beta_{gas} = 2(\beta_{tot} + 2)$. It is interesting to note that even though, in general, the solution in the inner region might differ from the solution in the outer region, as in the hydraulic jump (Watanabe, Putkaradze, & Bohr 2003; Hansen et al. 1997), then it happens that the connection in eq. (3) is the same everywhere (Hansen 2003).

If the mass in a given radial range is dominated by the gas itself, which may happen in the very inner region, then the solution is clearly $\beta_{gas} = -2$ (-4 or -6) if the polytropic index is $\gamma = 1$ ($3/2$ or $5/3$).

We emphasize that the result in eq. (3) is based on the simplifying assumption that both the gas density profile and the total mass profiles are power-laws, and therefore eq. (3) should only be seen as an approximation.

Various other possible behaviours for the gas profile have been proposed besides the one in eq. (3), e.g. that the gas density profile could follow that of the dark matter (Frenk et al. 1999)

$$\beta_{gas} = \beta_{tot}. \quad (4)$$

These simulations were considering cluster scales, where cooling is less relevant (see e.g. (Romeo et al. 2006)). Never the less, artificially created galaxies used in a range of N-body simulations (e.g. to investigate aspects of gas-cooling in a controlled manner (Kaufmann et al 2006)), are routinely constructed under the assumption in eq. (4). Another suggested behaviour of the gas density

is that it should be virtually independent of the local dark matter slope, and e.g. follow a β -profile (Sarazin 1986), where β_{gas} goes from zero in the center, to -3β in the outer region, which for the normal assumptions imply $\beta_{gas} \approx -2$ in the outer region.

3. The code and simulations

The code used for the simulations is a significantly improved version of the TreeSPH code, which has been used previously for galaxy formation simulations (Sommer-Larsen, Götz & Portinari 2003). The main improvements over the previous version are: (1) The “conservative” entropy equation solving scheme suggested by Springel & Hernquist (2002) has been adopted. (2) Non-instantaneous gas recycling and chemical evolution, tracing 10 elements (H, He, C, N, O, Mg, Si, S, Ca and Fe), has been incorporated in the code following Lia et al. (2002a,b); the algorithm includes supernovæ of type II and type Ia, and mass loss from stars of all masses. (3) Atomic radiative cooling depending both on the metal abundance of the gas and on the meta-galactic UV field, modeled after Haardt & Madau (1996) is invoked, as well as simplified treatment of radiative transfer, switching off the UV field where the gas becomes optically thick to Lyman limit photons on scales of ~ 1 kpc.

The formation and evolution of a total of 15 individual galaxies, known from previous work to become disk galaxies at $z=0$, was simulated with the above, significantly improved, TreeSPH code. At least two different numerical resolutions were used to simulate each galaxy. Moreover, many of the galaxies were also simulated with different physical prescriptions for the early ($z \gtrsim 4$) star-bursts (and related SNII driven energy feedback) found previously to be required, in order to produce realistic disk galaxies. The galaxies were selected to represent “field” galaxies (Sommer-Larsen, Götz & Portinari 2003), and span a range of characteristic circular speeds of $V_c \sim 100 - 330$ km/s, and virial masses of 6×10^{10} to $3 \times 10^{12} M_\odot$.

The galaxies (galaxy DM haloes) were selected from a cosmological, DM-only simulation of box-length $10 h^{-1} \text{Mpc}$ (comoving), and starting redshift $z_i=39$. The adopted cosmology was the flat Λ CDM model, with $(\Omega_M, \Omega_\Lambda)=(0.3,0.7)$.

Mass and force resolution was increased in Lagrangian regions enclosing the galaxies, and in these regions all DM particles were split into a DM particle and a gas (SPH) particle according to an adopted universal baryon fraction of $f_b=0.15$, in line with recent estimates.

In this paper, only results of two high-resolution simulations of two large disk galaxies will be presented (see Sommer-Larsen 2006 for details). Each simulation contains about 3×10^5 SPH+DM particles, and for the two simulations, $m_{\text{gas}} = m_* = 7.3 \times 10^5$ and $m_{\text{DM}} = 4.2 \times 10^6 h^{-1} M_\odot$, and $\epsilon_{\text{gas}} = \epsilon_* = 380$ and $\epsilon_{\text{DM}} = 680 h^{-1} \text{pc}$ ($h=0.65$). The gravity softening lengths were fixed in physical coordinates from $z=6$ to $z=0$, and in co-moving coordinates at earlier times. A Kroupa IMF was used in the simulations, and early rapid and self-propagating star-formation (sometimes dubbed “positive feedback”) was invoked (Sommer-Larsen, Götz & Portinari 2003).

The two galaxies have masses similar to those of M31 and the Milky Way, with characteristic circular velocities of $V_c = 245$ km/sec and 233 km/sec respectively. At $z=0$, each galaxy contains approximately 10^5 dark matter and 10^5 gas and star particles within the virial radius.

At any time there are satellites at various radii in these galaxies, which produce bumps in the total density profile. In order to reduce these bumps, we have co-added 5 frames with 1 Gyr spacing, corresponding to the period $z=0.3$ to $z=0$. No major merging was taking place during this period.

4. Comparing theory and simulations

In figures 1 and 2 we plot the logarithmic derivative of the gas density as a solid, blue line (with open circles) from the simulation. We emphasize that many more details are visible since we consider the derivative of the density profile. In the very central region the hot gas density profile becomes steep, because the density is calculated including hot gas particles very near the cold, high-density gas disk (i.e., a numerical effect). If these near disk hot particles are excluded, the density slope of the hot gas goes towards zero near the center.

Outside $\log(r)=1.4$ the gas slope falls slowly from -1 in the central region, to -3 in the outer region near $\log(r)=2.4$. The virial radius is ap-

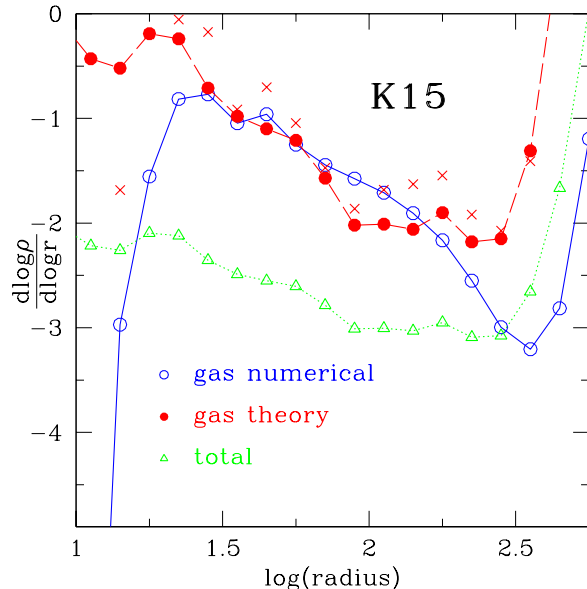


Fig. 1.— Logarithmic derivative of the density profiles of gas and total matter as function of radius. The solid blue line (open circles) is the simulated gas density profile (the logarithmic derivative), and the green dotted line (open triangles) is the simulated total density profile. The red dashed line (filled circles) is the theoretical prediction from eq. (3) using $\gamma = 3/2$, and the red crosses are using the simulated value of $\gamma(r)$. This galaxy has $V_c = 245$ km/sec. Inside $\log(r) = 1.4$ the numerical gas density slope is dominated by the cold high-density gas disk. Outside $\log(r) = 2.5$ a neighbouring galaxy affects the density slope.

proximately 250 kpc, corresponding to $\log(r)=2.4$. Further out, for galaxy K15, the presence of a neighbouring galaxy causes the total and hot gas density profiles to flatten.

Let us now compare this behaviour of the density profile to the theoretical predictions. The simulated behaviour of the gas profile is clearly very different from a beta-profile, which should go from zero in the central region to roughly -2 further out. It therefore appears that the hot gas in dynamically old structures, like a galaxy, is not well described by a β profile.

We also plot the total density as a green, dotted line (with open triangles). According to the Santa Barbara comparison (Frenk et al. 1999), the solid,

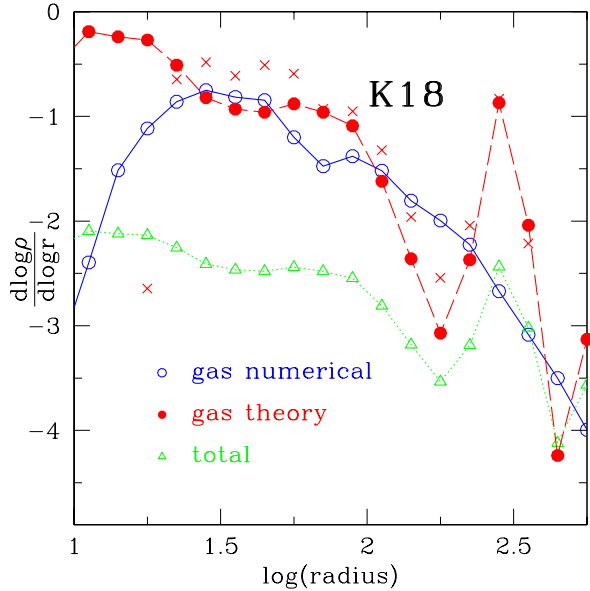


Fig. 2.— Logarithmic derivative of the density profiles of gas and total matter as function of radius. The solid blue line (open circles) is the simulated gas density profile (the logarithmic derivative), and the green dotted line (open triangles) is the simulated total density profile. The red dashed line (filled circles) is the theoretical prediction from eq. (3) using $\gamma = 3/2$, and the red crosses are using the simulated value of $\gamma(r)$. This galaxy has $V_c = 233$ km/sec. Inside $\log(r) = 1.4$ the numerical gas density slope is dominated by the cold high-density gas disk. Near the virial radius, $\log(r) = 2.4$, the effect of infalling substructure is clearly seen as a bump in the total density slope.

blue line and the green dotted line could be similar. It is clear that the behaviour of derivatives of the total and gas density are very different everywhere within the virial radius, since the gas does not follow $\beta_{gas} = \beta_{tot}$, though this is often considered as a realistic initial condition for galaxy models. Our results indicate that such initial conditions are not in agreement with results for galaxies formed in Λ CDM cosmological simulations.

As red dashed line (with solid circles) we have the prediction from eq. (3). There is impressive agreement for radii outside the central disk region at $\log(r)=1.4$ to the virial radius. The obvious in-

terpretation is that the hot gas is sufficiently close to hydrostatic equilibrium.

From a practical point of view, this result gives us a very strong handle on how to set up initial condition for realistic galaxies for numerical experiments. One should simply use the total density profile (typically dominated by the underlying dark matter distribution) together with eq. (3).

For the comparisons above we have used $\gamma = 3/2$. From the simulations we naturally have $\gamma(r)$ in each radial bin from eq. (2), and we find that $\gamma = 3/2$ is a very good approximation in the entire region considered, namely $1.4 < \log(r) < 2.4$. In the figures we also present (as red crosses) the prediction from eq. (3) when using the actual value of $\gamma(r)$, and we see that there is very little difference from simply using $\gamma = 3/2$.

4.1. Additional aspects

One seemingly disturbing aspect of eq. (3) is that if the total density slope becomes more shallow than -2, then the gas density profile gets a positive sign. We find that it is a remarkable conspiracy that the total density profile indeed remains as steep as -2 in the virialized region (see green open triangles in the figures).

In the very central region the gas density is dominated by the cold gas disk. The predictions for a disk-profile is different than the predictions for a spherical distribution in eq. (3), and the disk predictions is approximately $d \log \rho / d \log r \approx -2$, which is in rough agreement with the numerical findings (see blue, open circles for $\log(r) < 1.4$).

It was suggested that the tangential velocity distribution might have a transition from the inner region to the outer region of the form

$$v_{\tan} = v_{\alpha} \left(\frac{r}{r_{\alpha}} \right)^{\alpha}, \quad (5)$$

where α should go from unity in the inner region, to -2 in the outer region (Hansen & Stadel 2003). We find that the tangential velocity is well fitted with the shape $v_{\tan} = \exp(-r^{2.3})$ everywhere in the resolved region. This simply shows, that the assumption of a power-law for the rotational gas velocity is not good. Furthermore, the gas is approximately in hydrostatic equilibrium, and has only a small radial velocity component in the central region where cooling is most important. We

hope to investigate the details of the radial velocity and an exponential tangential velocity in the future.

5. CONCLUSIONS

Standard galaxy formation scenarios predict that the central cold gas-disk and stars are surrounded by an extended halo of hot gas. We investigate quantitatively the density profile of this gas-halo. We find that results of cosmological Λ CDM N-body/hydrodynamical simulations of the formation and evolution of galaxies, and analytical solutions to the fundamental gas equations are in remarkable agreement. We find that the gas density slope (the logarithmic derivative) is a non-trivial function of the slope of the total matter, expressed through eq. (3). This equation is useful when constructing realistic galaxies for controlled numerical experiments.

SHH is supported by the Swiss National Foundation. The Dark Cosmology Centre is funded by the DNRF.

REFERENCES

- Frenk, C. S. et al. 1999, arXiv:astro-ph/9906160.
- Haardt, F. & Madau, P. 1996, *Astrophys. J.* 461, 20
- Hansen, S. H., Horlück, S., Zauner, D., Dimon, P., Ellegaard, C. and Creagh, S. C. 1997, *Phys. Rev. E* 55, 7048
- Hansen, S. H. & Stadel, J. 2003, *Astrophys. J.* 595, L37
- Hansen, S. H. 2003, Proceedings of Blois conference, arXiv:astro-ph/0310302
- Kaufmann, T., Mayer, L., Wadsley, J., Stadel, J. & Moore, B. 2006, *MNRAS* to appear, astro-ph/0601115
- Lia, C., Portinari, L., Carraro, G. 2002, *MNRAS*, 330, 821
- Lia, C., Portinari, L., Carraro, G. 2002, *MNRAS*, 335, 864
- Matsushita 2001, *ApJ*, 547, 693
- Pedersen, K. P. et al. 2006, *New Astronomy* 11, 465
- Romeo, A.D., Sommer-Larsen, J., Portinari, L. & Antonuccio-Delogu, V. 2006 *MNRAS*, in press (astro-ph/0509504)
- Sarazin, C. L. 1986, *Reviews of Modern Physics*, 58, 1
- Springel, V. & Hernquist 2002, *MNRAS*, 333, 649
- Sommer-Larsen, J., Götz, M. & Portinari, L. 2003, *ApJ*, 596, 46
- Sommer-Larsen, J. 2006, *ApJ*, in press (astro-ph/0602595)
- Watanabe, S., Putkaradze, V. and Bohr, T. 2003, *J. Fluid Mech.*, 480, 233
- White, S.D.M. & Frenk, C.S. 1991, *ApJ* 379, 52